J. Min. Metall. Sect. B-Metall. 61 (1) (2025) 1 - 9

Journal of Mining and Metallurgy, Section B: Metallurgy

THE IMPACT OF HOT ROLLING TEMPERATURE ON THE MICROSTRUCTURE AND CORROSION RESISTANCE OF SUPER DUPLEX STAINLESS STEEL, USED FOR COATING MILD STEEL IN SEAWATER ENVIRONMENTS

L. Naffat [a,*], M.S. Anwar [a], P.A. Paristiawan [a], A.N. Syahid [a], R.N. Hakim [a], Y. Lestari [a], M. Perkasa [b], K. Prijono [c]

[a] Research Center for Metallurgy, National Research and Innovation Agency (BRIN), South Tangerang, Jakarta, Indonesia
[b] Laboratory of Structural Strength, National Research and Innovation Agency (BRIN), South Tangerang, Jakarta, Indonesia
[c] Advanced Chemical and Advanced Physics Imaging Laboratory, National Research and Innovation Agency (BRIN), South Tangerang, Jakarta, Indonesia

(Received 26 September 2024; Accepted 27 December 2024)

Abstract

A new material that can be used to replace single steel in high-strength tanks is mild steel cladding Super Duplex Stainless Steel (SDSS). The method of producing multilayer Super Duplex Stainless Steel (SDSS) is the cladding of mild steel Many processes are carried out such as welding *Plasma Direct Energy Deposition (DED), laser, and electro-slag strip. In the manufacturing industry, hot rolling is a simple process. Because the procedure is quick and uses inexpensive, traditional equipment, it is referred to as a simple method. The use of seawater was chosen because salty conditions favour corrosion. In this work, the effects of temperatures of 900°C, 1000°C, and 1050°C on the microstructure and corrosion resistance of hot rolled materials are investigated. The investigation of corrosion resistance by examining the microstructure and material properties using metallography, X-ray diffraction, Electrochemical Impedance Spectroscopy (EIS), and Scanning Electron Microscope (SEM) is the main goal of this work. The results of the study demonstrated that when the hot rolling temperature was increased, carburization and decarburization occurred and the corrosion resistance decreased.*

Keyword: *SDSS; Mild steel; Hot rolling; Carburization; Decarburization*

1. Introduction

In industrial settings, carbon steel is often prone to corrosion, and a high level of corrosion resistance is necessary for both economic and secure operation. Crude oil is used in the oil and gas sector because it contains specific chemical constituents that can acceleratecorrosion, like sulfur, nitrogen, and aromatic resins. Using organic or inorganic inhibitors, which shield the steel surface by creating a passive protective layer is the most common method of increasing corrosion resistance [1, 2].

A unique iron alloy known as duplex stainless steel comprises balanced phases of austenite (γ) and ferrite (δ) in its microstructure. In situations containing acids, acidic chlorides, seawater, and chemicals, this two-phase structure results in a steel with excellent strength, toughness, and corrosion resistance [2-4]. The use of super duplex stainless steel has increased in areas that are extremely corrosive, such as pulp and paper manufacturing, heat exchangers, chemical storage tanks, and oil and gas infrastructure. For the uses listed above, corrosion-resistant duplex stainless steel alloys are more corrosion-resistant than low-carbon steels, albeit are associated with significantly higher material costs [5].

In previous studies on the production of multilayer stainless steel and carbon steel, various methods have been used, namely welding methods [3, 6, 7, 8] Plasma Direct Energy Deposition (DED) [9], laser [10-13], and electro-slag strip [14]. The hot and cold rolling processes used for super duplex steel do not significantly affect the material's surface. Nevertheless, cold rolling is preferable than hot rolling for corrosion resistance [15]. Low-carbon steel

Corresponding author: lusianand@yahoo.com

https://doi.org/10.2298/JMMB240926001L

is hot rolled to obtain better mechanical properties, whereby the mechanical properties are improved compared to cold working [16].

Although the surface of super duplex steel is not significantly damaged during either the hot or cold rolling, the cold rolling method improves corrosion resistance over the hot rolling process [17]. To obtain better mechanical properties, mild steel is hot rolled which improves the mechanical properties compared to cold working [18].

The improvement of mechanical qualities and corrosion resistance is the goal of creating multilayers between two different materials [19]. Compared to coldforming, the corrosion resistance of multilayer duplex made of carbon steel that has been hot rolled and aged leads to precipitation [20]. Meanwhile, corrosion can be produced effectively using the electro slag strip method with different solutions [21]

The aim of this study is to investigate the corrosion resistance of Super Duplex Stainless Steel (SDSS) - multilayer structural steel systems during the hot rolling process in saline environment. The focus of this study is to investigate the corrosion resistance using microstructure tests and material properties such as scanning electron microscope (SEM), metallography, X-ray diffraction and electrochemical impedance spectroscopy (EIS).

2. Materials and Methods

Superduplex and low carbon steel materials were cut to the same size, and to prevent the two materials from shifting after rolling, the ends of the materials were welded together. Then, employing temperatures of 900°C, 1000°C, and 1050°C, the hot rolling process was completed. This research experiment can be seen in the schematic diagram in Figure 1.

Table 1 shows the factors used in this investigation. To facilitate the testing, the material was chopped after the temperature was changed, and then mounted with resin. Sandpaper with a roughness of 120, 240, 400, 600, 800, 1000, and 1200, 1500, 2000 was used to grind the samples. The JEOL JSM IT-200 LA was then used to conduct the test using a scanning electron microscope (SEM). Meanwhile, the Panalytical Empiren is used for XRD. After polishing the sample with cloth disks containing diamond paste in a size of 0.3m, the sample was etched with Kalling's solution to view its microstructure. An Olympus microscope, which is used for metallography, was one of the tools used Using a test electrolyte of 5% NaCl aqueous solution, all electrochemical experiments were conducted in a three-electrode electrochemical cell. Coated specimens served as working electrode, while graphite plates and saturated calomel electrodes (SCE) served as counter and reference electrodes. Potentiostat/galvanostat/ZRA Gamry 3000 and other test instruments were used.

Table 2 illustrates that carbon steel materials falls under the ASTM SA 210A1 or ASTM 213 standards, which are frequently applied to pipes, such as those made of austenitic and ferritic steel for superheaters, heat-exchanger tubes, and boilers [22]. As a super duplex stainless steel (SDSS) material, it is mostly

Table 1. *Research variables*

Sample/code sample	Temperature Rolling (°C)
Mild steel (1)	-
SDSS (2)	-
Cladding (3)	900
Cladding (4)	1000
Cladding (5)	1050

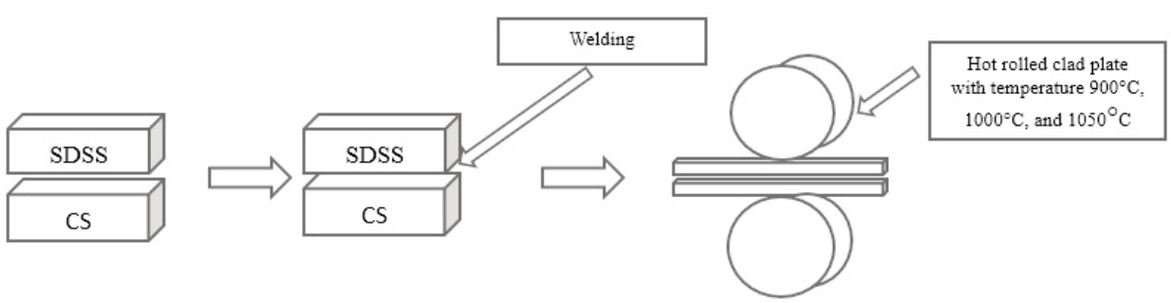

Figure 1. *Schematic diagram for hot rolling*

Table 2. *Chemical composition of mild steel and SDSS (wt%)*

Material	C	Si	Mn	Cr	Mo	Ni	P	S	Fe
Mild steel	0.14	0.16	0.69	0.11	0.024	0.097	<0.01	<0.01	bal
SDSS	0.01	0.37	0.34	24.92	3.87	6.36	<0.01	<0.005	bal

utilized in the oil and gas industry, particularly for offshore platforms, heat exchangers, structural elements, and architectural elements. Type UNS: S32750 is a variant of the stainless steel alloy [23].

3. Result and Discussion

3.1. Microstructures

The outcomes of the metallographic testing with Kalling's etching are shown in Figure 2. Mild steel, the decarburization area, the SDSS, and the carburization area are the four components of the microstructure study of samples with variations in hot rolling temperatures of 900°C, 1000°C, and 1050°C. High temperatures cause metallurgical bonding, or the reciprocal diffusion of elements [24]. Figure 2(a) shows that the decarburization layer formed on the mild steel side is not particularly apparent, and the carburization layer on the SDSS side is not very thick. The carburization and decarburization layers are thicker in Figure 2(b) from both the mild steel and SDSS sides than in Figure 2(a), while the carburization layer is thinner in Figure 2(c) than in Figure 2(b). The cladding contact exhibits a uniform and clearly visible decarburization layer on the mild steel side [25]. The diffusion of components during heating results in carburization zones and decarburization [26]. The initial driving force for the diffusion of elements is provided by the considerable differences in the amount of C, Cr, Fe, and other elements between mild steel and SDSS. Ferrite and pearlite make up the structure of the mild steel region. The carbon atoms from the mild steel close to the interface diffuse across the layer boundary to the SDSS side during the heating process in the decarburization zone, reducing the carbon content in the pearlite and causes it to change to a ferrite structure when the rolling temperature is increased. Therefore, only a coarse ferrite structure is present in the decarbonization zone as a result. C atoms are added to the SDSS side in the carburization zone, whilst Cr atoms from the SDSS diffuse into the mild steel in the vicinity of the interface. In the cladding layer, SDSS starts to change into a thick austenite structure due to a rise in the element C, which promotes austenite, and a decrease in the element Cr, which promotes ferrite. Element diffusion has little effect on the ferrite + austenite structure located far from the cladding. When the heating temperature increases, the grain size, decarburization zone, and carburization zone become larger [27].

Figure 3(a) illustrates how the surface of SDSS is corroded, as indicated by the black color present; on the surface of low-carbon steel, the corrosion product takes the form of powder. Corrosion also occurs on the cladding, but is not as bad as on the surface.

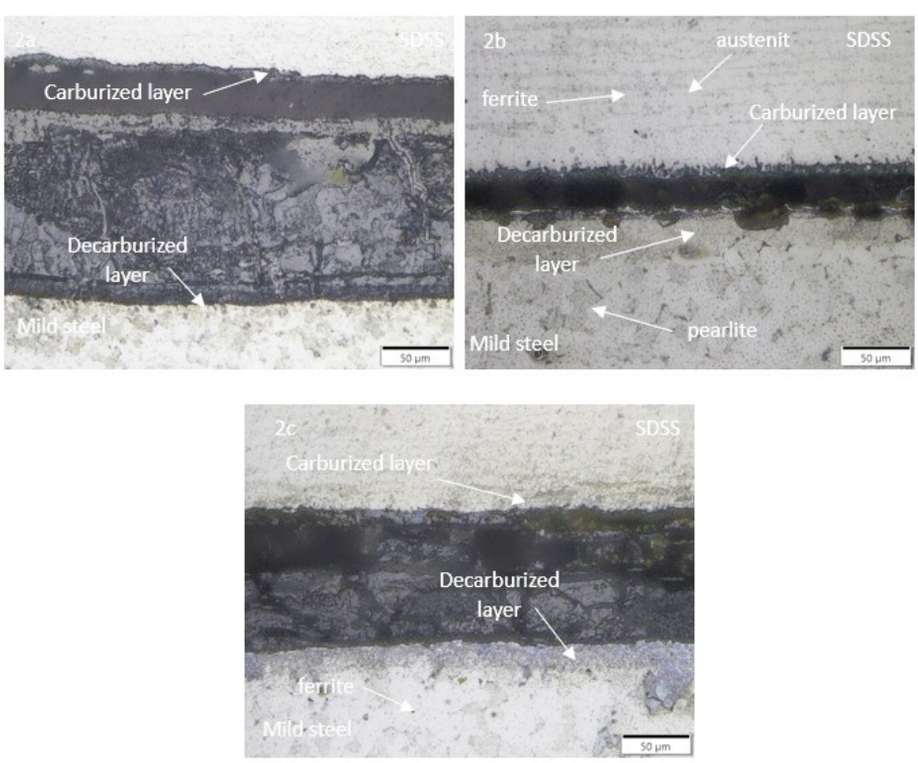

Figure 2. *Results of metallographic test; the temperatures at which hot rolling occurs are (2a) 900°C, (2b) 1000°C, and (2c) 1050°C*

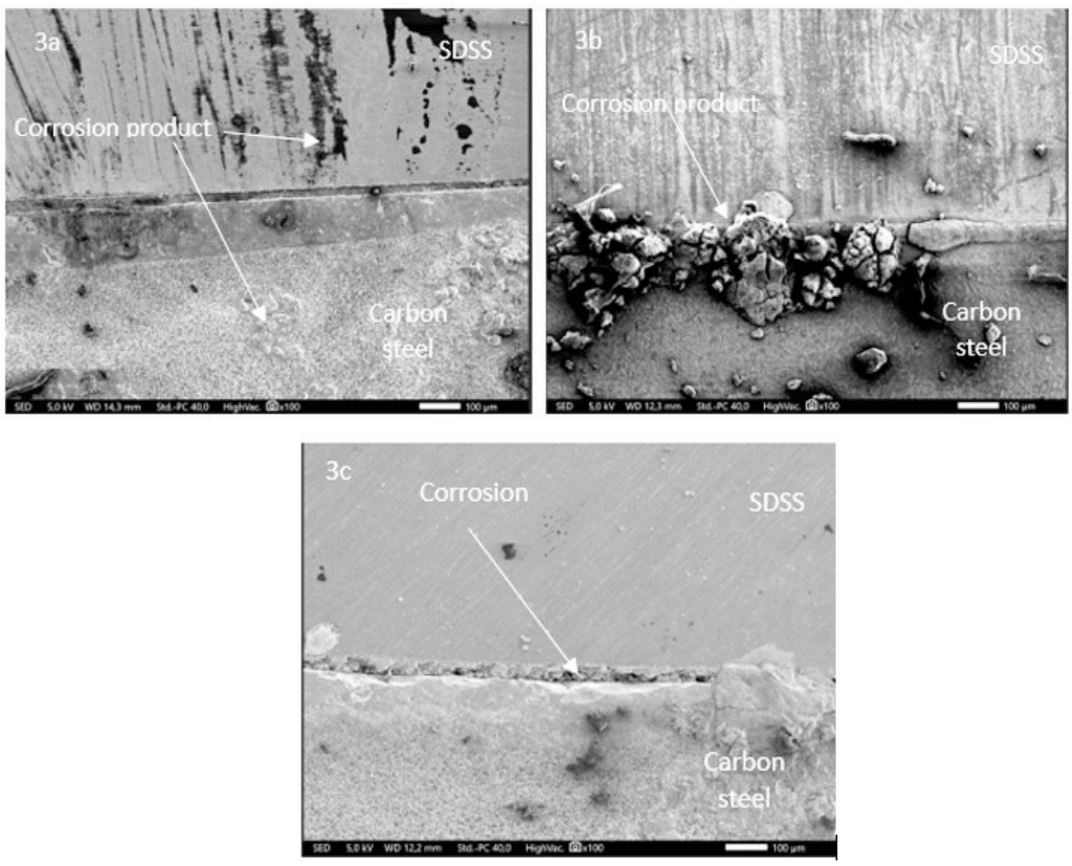

Figure 3. *SEM results after the hot rolling process, (3a) rolling temperature 900°C, (3b) rolling temperature 1000°C, (3c) rolling temperature 1050°C*

Figure 3b shows that the corrosion on the cladding occurs on the low carbon steel side, but compared to the low carbon steel side, the corrosion on the SDSS surface is not as severe.

Figure 3c shows the corrosion on the low-carbon steel surface and the cladding. The corrosion appears porous and eats away part of the cladding. The corrosion that develops on the low carbon steel surface further from the cladding is nearly identical to that shown in Figure 3a. As explained in the microstructure results, this damage is caused by the decarburization process in the cladding, resulting in corrosion products and damaged cladding.

3.2. XRD result

The XRD graph in Figure 4, created with Macth! Software, shows that the cubic crystal form with the lattice parameter (a) 3.6710 Å has Fe peaks (111), (313), and (400) at a hot rolling temperature of 900°C. The peaks formed at 1000°C hot rolling temperature are (101) and (202), with a cubic lattice parameter (a) of 2.8714 Å; at 1050°C hot rolling temperature, the peak is formed (101), with a lattice parameter (a) of 3.5140 Å. The size of the lattice parameter varies at different hot rolling temperatures, as can be observed here.

Iron A has two crystal structures: FCC (Face Body Center) and BCC (Body Cubic Center). In contrast to the FCC structure, the iron atoms in the BCC crystal structure have more mobility to travel and diffuse. This is because the atomic arrangement in the BCC structure is less dense and more open, with larger interstitial gaps between the atoms. This facilitates the easier diffusion and mobility of the iron atoms within the crystal lattice. In comparison, the iron atom arrangement in the FCC crystal structure is denser and has smaller interstitial spaces. In comparison to BCC iron, this restricted atomic mobility makes it more difficult for the iron atoms to diffuse through the lattice, leading to a reduced self-diffusion coefficient [28].

From the Match! database a hot rolling temperature of 900 was used to generate the space group Fm-3m (225). At 910°C, iron exhibits a Face Cubic Center (FCC) structure [28, 29] The resulting space group is lm-3m with a Body Cubic Center (BCC) structure at 1000°C

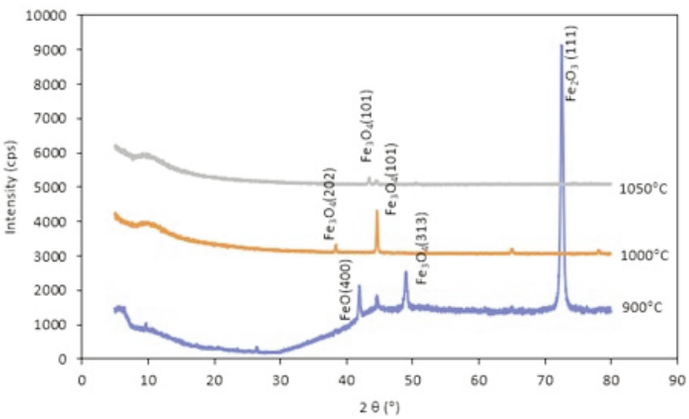

Figure 4. *XRD Pattern of SDSS mild steel cladding with hot rolling temperature 900°C, 1000°C, and 1050°C*

The crystal structure returns to the Face Cubic Center (FCC) around 1050°C [29]. This variation results from anisotropic iron's ability to form distinct crystal structures at various temperatures before returning to its original form.

3.3. Electrochemical properties

The curve of the multilayer test for carbon steel and SDSS at room temperature using a 5% NaCl solution is shown in Figure 5. In this instance, the NaCl solution was chosen since it is a solution used for multilayer corrosion testing in seawater on SDSS and mild steel [30, 31].

The corrosion mechanism in the super duplex mild steel cladding is illustrated in Figure 5 by the potential-dynamic curve of the polarization of the cladding caused by changes in hot rolling temperature in a 5% NaCl solution. In comparison to the change in hot rolling temperature, the resulting curve is not that different.

The capacity of a metal to react electrochemically with its surroundings is known as corrosion potential (Ecorr), whereas the quantity of electron movement associated with the corrosion rate in steel is known as its corrosion current (I_{corr}) [32]. Table 3 shows that sample 1 has an I_{corr} of 7.216 x 10^{-6} A/cm^2 and a corrosion rate of 88.77 x 10^{-3} mmpy. The E_{corr} of sample 1 is -647.1 mV. E_{corr} was -615.7 mV in sample 2, I_{corr} was 3.571 x 10^{-6} A/cm^2 and the corrosion rate was 41.46 x 10^{-3} mmpy. For sample 3, E_{corr} was -1.023 mV with I_{corr} being 68.10 x 10^{-6} A/cm^2 and the corrosion rate being 790.5 x 10^{-3} mmpy. At a hot rolling temperature of 1050°C, sample 3 readily reacts

Table 3. *Electrochemical parameters of potentiodynamic test resultshot rolling temperature 900°C, 1000°C, and 1050°C*

Sample	E_{corr} (mV)	I_{corr} (A/cm^2)	Corrosion rate (mmpy)
1	-647.1	7.216 x 10^{-6}	88.77 x 10^{-3}
2	-615.7	3.571 x 10^{-6}	41.46 x 10^{-3}
3	-1.023	68.10 x 10^{-6}	790.5 x 10^{-3}

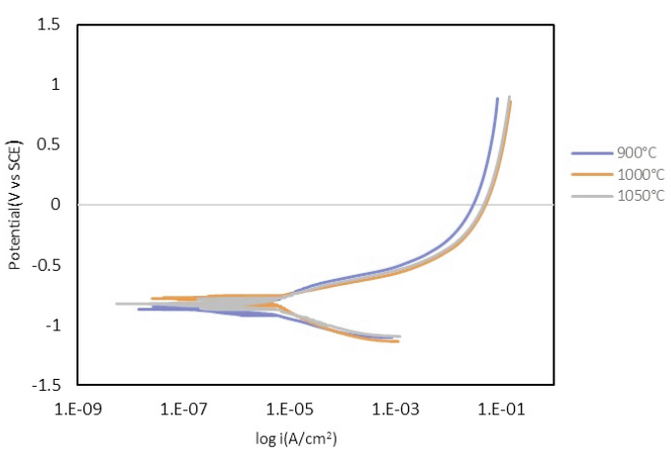

Figure 5. *The potentiodynamic polarization curve of super duplex mild steel cladding by variation of hot rolling temperature in 5% NaCl solution*

electrochemically with its surroundings and has a higher electron mobility, which leads to a rapid corrosion rate, according to the results [33].

Figure 6. shows the electrochemical impedance spectra (EIS) of mild steel and multilayer SDSS after hot rolling. It also shows the equivalent circuit model for fitting the EIS data at open circuit potential in 5% NaCl, as well as the Nyquist and Bode-modulus-phase plots.

The Nyquist plot of the EIS shows that the semi-circular curve occurs for all steel grades in the high to low-frequency range. This indicates that all steel grades have two resistances, namely the solution resistance (Ru) and charge transfer resistance (Rp). The circuit used for modeling the Nyquist plot of the EIS is a simple Randless circuit model [34]. The equivalent circuit used for modeling the EIS results is shown in Figure 6 (c). The equivalent circuit used is the Constant Phase Element (CPE) equivalent circuit consisting of Ru, Rp, Yo, and alpha elements.

Based on Figure 4(a), the Nyquist curve with hot rolling temperature variations of 900°C, 1000°C, and 1050°C shows that diffusion happens at very low frequencies, meaning that the oxide layer formed is thin and discontinuous, allowing corrosion species to diffuse to the metal surface [35]. The rate of corrosion increases with increasing hot rolling temperature (Table 3). Hot rolling at 1050°C results in a decrease in corrosion resistance and a smaller curve diameter on the Nyquist curve than rolling at 900°C and 1000°C, which is followed by a drop in the Rp value (Table 4). This suggests that the value of polarization resistance decreases with increasing hot rolling temperature, and the corrosion rate increasescorrosion. The oxide layer that forms and has protective properties is represented by the high diameter of the Nyquist curve. On the other hand, the decreasing diameter of the Nyquist curve suggests that the oxide formed is not continuous and that there are gaps or pores that allow diffusion to occur, which again increases the rate of corrosion [36] The magnitude of the impedance with phase shift is represented by the bode plot in Figure 5(b). The impedance increases at low frequencies as the hot rolling temperature increases (at low frequencies, it approaches the ohmic resistance, i.e.the charge transfer resistance) [20]. At higher hot rolling temperatures, a more unstable layeris formed.

Table 3. *Result of EIS fit for SDSS cladd mild steel in the 5% NaCl solution*

Sample	Ru	Rp	Yo	Alpha
	(W/cm^2)	(W/cm^2)	($\mu S/cm^2 s^a$)	
1	10.32	$2.384e^3$	$695.1e^{-6}$	$696.8e^{-3}$
2	6.655	$1.873e^3$	$520.6e^{-6}$	$800.5e^{-3}$
3	7.103	$1.437e^3$	$1.029e^{-3}$	$738.1e^{-3}$

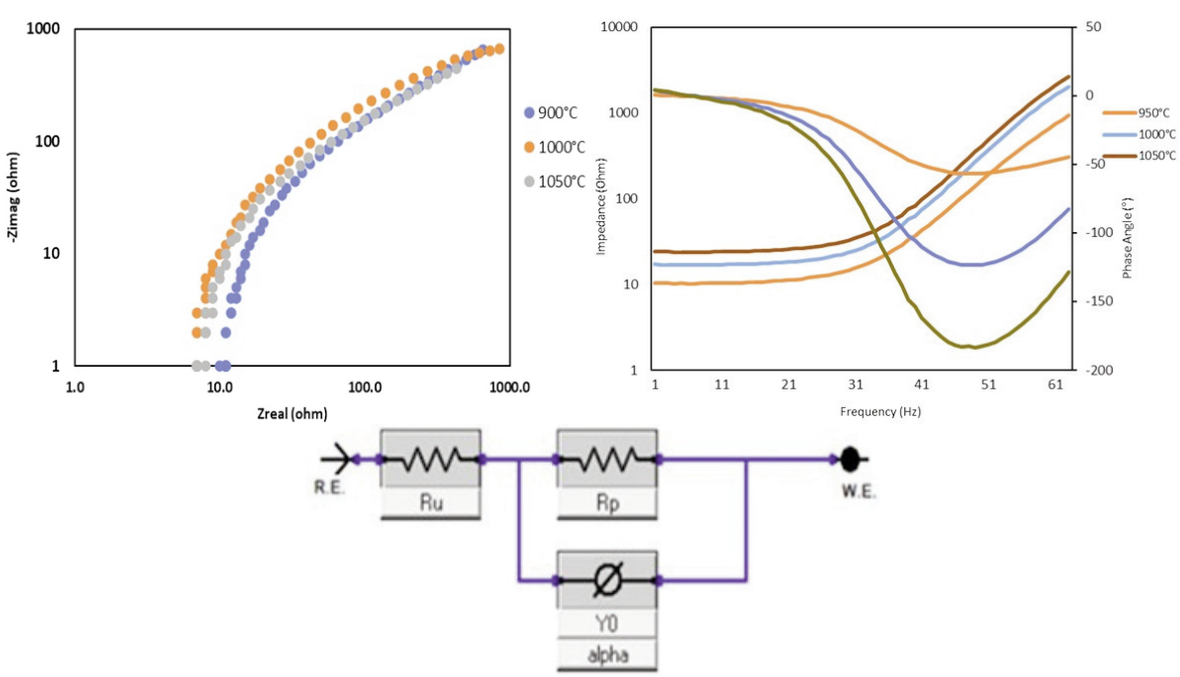

Figure 6. *Eletrochemical impedans spectra of multilayer SDSS and baja karbon with variation temperature hot rolling (a) Nyquist plot (b) Bode plot (c) equivalent circuit model for EIS data fitting at open circuit potential in 5% NaCl*

4. Conclusions

The results of the study indicate that the cladding process of mild steel and SDSS by hot rolling at temperatures of 900°C, 1000°C, and 1050°C results in a microstructure that varies between the mild steel and SDSS material sides and causes carburization and decarburization by diffusion. A temperature of 900°C results in a crystal structure that is FCC, at 1000°C it is BCC, and at 1050°C it is FCC. Ferrous exhibits anisotropic characteristics, meaning that its crystal structure varies with temperature. When the hot rolling temperature reaches 1050°C, corrosion resistance starts to decrease with increasingtemperature, which can berecognized by theincreasing corrosion.

Acknowledgment

This work was supported by the Grant of Research Organization for Nanotechnology and Materials, National Research and Innovation Agency (BRIN) of the Republic of Indonesia.

Conflict of interest

The authors declare that they have no known conflicts of interest

Author contributions

Lusiana: conceptualization, experimental work, investigation, resources, writing - original draft, writing - review and editing, and visualisation. Moch.Syaiful Anwar: supervision, visualization and validation. Permana Andi Paristiawan, Mustasyar Perkasa: technical support and process hot rolling. Adi Noer Syahid: technical support and help with SEM characterisation. Rahma Nisa Hakim: technical support and help with Microstructure characterisation. Yulinda Lestari: technical support and help with Elektrochemical characterisation. Kusdi Prijono: technical support and help with XRD characterisation.

Data Availability Statement

Data will be made available on request.

References

[1] D.H. Abdeen, M. El Hachach, M. Koc, M.A. Atieh, A review on the corrosion behaviour of nanocoatings on metallic substrates, Materials, 12 (2019) 1-42. https://doi.org/10.3390/ma12020210

[2] Y. Han, Z.H. Liu, C.B. Wu, Y. Zhao, G.Q. Zu, W.W. Zhu, X. Ran, A short review on the role of alloying elements in duplex stainless steels, Tungsten, 5 (2023) 419–439. https://doi.org/10.1007/s42864-022-00168-z

[3] A.A. Mudha, H.D. Shashikala, H.S. Nagaraja, Corrosion protection of low-cost carbon steel with SS-309Mo and Inconel-625 bimetallic weld overlay, Material Research Express, 6 (2019) 1-17. https://doi.org/10.1088/2053-1591/aafba6

[4] A. Amudha, H.S. Nagaraja, H.D. Shashikala, Finite element analysis of thermal residual stresses in SS-309Mo and Inconel-625 multilayer weld deposition on low carbon steel, International Journal of Fatigue, 127 (2019) 338–344. https://doi.org/10.1016/j.ijfatigue.2019.06.014

[5] R. Francis, G. Byrne, Duplex stainless steels—alloys for the 21st century, Metals, 11 (2021) 1-23. https://doi.org/10.3390/met11050836

[6] B. Heider, M. Oechsner, U. Reisgen, J. Ellermeier, T. Engler, G. Andersohn, R. Sharma, E. Gonzalez Olivares, E. Zokoll, Corrosion resistance and microstructure of welded duplex stainless steel surface layers on gray cast iron, Journal of Thermal Spray Technology, 29 (2020) 825–842. https://doi.org/ 10.1007/s11666-020-01003-y

[7] E. Atindra Joshi, S. Parkash, E. Manoj Kumar, Study of Mechanical Properties, Microstructure and corrosion behavior of super duplex-2594 weld overlay on carbon steel substrate by smaw, Journal of Engineering Research and Application, 8 (2018) 65–70. https://doi.org/ 10.9790/9622-0807016570

[8] L. Wanga, Y. Ding, Q. Lub, Z. Guo, Y. Liua, Z. Cui, Microstructure and corrosion behavior of welded joint between 2507 super duplex stainless steel and E690 low alloy steel, Corrosion Communications, 11 (2023) 1-11. https://doi.org/10.1016/j.corcom.2022.08.005

[9] S. Yang, K. Cooke, H. Sun, X. Li, K. Lin, H. Dong, Development of advanced duplex surface systems by combining CrAlN multilayer coatings with plasma nitrided steel substrates, Surface and Coatings Technology, 236 (2013) 2–7. https://doi.org/10.1016/j.surfcoat.2013.07.017

[10] C.P. Paul, H. Alemohammad, E. Toyserkani, A. Khajepour, S. Corbin, Cladding of WC-12 Co on low carbon steel using a pulsed Nd:YAG laser, Materials Science and Engineering, 464 (2007) 170–176. https://doi.org/ 10.1016/j.msea.2007.01.132.

[11] K.T. Laitinen, H. Korhonen, J.T.T. Leskinen, A. Koistinen, R. Lappalainen, Improved multilayer coatings by combined use of electrochemical and ultra-short pulsed laser deposition techniques, Surface and Coatings Technology, 300 (2016) 58–66. https://doi.org/ 10.1016/j.surfcoat.2016.05.031

[12] P. Murkute, S. Pasebani, O. Burkan Isgor, Metallurgical and electrochemical properties of super duplex stainless steel clads on low carbon steel substrate produced with laser powder bed fusion, Scientific Reports, 10 (2020) 1-19. https://doi.org/10.1038/s41598-020-67249-2

[13] J. Liu, H. Liu, X. Tian, H. Yang, J. Hao, Microstructural evolution and corrosion properties of Ni-based alloy coatings fabricated by multi-layer laser cladding on cast iron, Journal of Alloys and Compounds, 822 (2020) 1-11. https://doi.org/10.1016/j.jallcom.2020.153708

[14] A.M. Bogatu, C. Rontescu, R.C. Diacu,, D-T. Cicic,

Research regarding strip cladding of heat-resistant SA 387 Gr.11Cl.2 steel type, Materials Science and Engineering, 1182 (2021) 1-6. https://doi.org/10.1088/1757-899X/1182/1/012008

[15] T. Gao, J. Wang, Q. Sun, P. Han, Corrosion behavior difference in initial period for hot-rolled and cold-rolled 2205 duplex stainless steels, Metals, 8 (2018) 2-13. https://doi.org/ 10.3390/met8060407

[16] A.A. Mudha, H.D. Shashikala, H.S. Nagaraja, Corrosion protection of low-cost carbon steel with SS-309Mo and Inconel-625 bimetallic weld overlay, Material Research Express, 6 (2019) 1-17. https://doi.org/ 10.1088/2053-1591/aafba6

[17] M.H.E. Seshweni, A. Moloto, S. Aribo, S.R. Oke, O.O. Ige, P.A. Olubambi, Influence of cold and hot rolling on the corrosion behaviour of duplex stainless steels in mine water environment, Materials Today, Proceedings (2019) 1-4. https://doi.org/10.1016/j.matpr.2019.12.323

[18] M. Herrmann, C. Schenck, H. Leopold, B. Kuhfuss, Material improvement of mild steel S355J2C by hot rotary swaging, Procedia Manufacturing, 47 (2020) 282–287. https://doi.org/ 10.1016/j.promfg.2020.04.224

[19] G. Yuan, P. Han, X. Zhu, Z. Jiang, X. Wang, Fabrication of a composite material of high-chromium cast iron dispersed in low-carbon steel by hot-rolling process, Steel Research International, 92 (2021) 1-10. https://doi.org/10.1002/srin.202100001

[20] Y. Han, J. Shi, L. Xu, W. Q. Cao, H. Dong, Effect of hot rolling temperature on grain size and precipitation hardening in a Ti-microalloyed low-carbon martensitic steel, Materials Science and Engineering: A, 553 (2012) 192–199. https://doi.org/10.1016/j.msea.2012.06.015

[21] D.S. Kahar, K.B. Pai, Corrosion behavior of electro-slag strip cladded weld overlays in different acid solutions, 3 (2013) 2620-2627, ISSN: 2248-9622.

[22] Designation: A213/A213M − 13 Standard Specification for Seamless Ferritic and Austenitic Alloy-Steel Boiler, Superheater, and Heat-Exchanger Tubes, ASTM International, 0101 (2018) 1-14.

[23] E.M. Cojocaru, D. Raducanu, A. Nocivin, V. D. Cojocaru, Influence of ageing treatment temperature and duration on σ-phase precipitation and mechanical properties of UNS S32750 SDSS alloy, Journal of Advanced Research, 30 (2021) 53–61. https://doi.org/ 10.1016/j.jare.2020.11.005

[24] K.O. Cooke, A.M. Atieh, Current trends in dissimilar diffusion bonding of titanium alloys to stainless steels, aluminium and magnesium, Journal of Manufacturing and Materials Processing, 4 (2020) 1-22. https://doi.org/ 10.3390/jmmp4020039

[25] Y. Yang, Z. Jiang, X. Liu, J. Sun, W. Wang, Enhanced interfacial strength and ductility of stainless steel/carbon steel laminated composite by heterogenous lamella structure, Journal of Materials Research and Technology, 18 (2022) 4846–4858. https://doi.org/ 10.1016/j.jmrt.2022.04.057

[26] Y. Yang, Z. Jiang, Y. Chen, X. Liu, J. Sun, W. Wang, Interfacial microstructure and strengthening mechanism of stainless steel/carbon steel laminated composite fabricated by liquid-solid bonding and hot rolling, Journal of Materials Research and Technology, 191 (2022), 4846-4858.

https://doi.org/ 10.1016/j.matchar.2022.112122

[27] F. Xiao, D. Wang, Z. Gao, L. Zhou, Effect of heating process on microstructure and properties of 2205/Q235B composite interface, Metals, 9 (2019) 2-17. https://doi.org/10.3390/met9101027

[28] K.T. Moore, D.E. Laughlin, P. Söderlind, A. J. Schwartz, Incorporating anisotropic electronic structure in crystallographic determination of complex metals: Iron and plutonium, Philosophical Magazine, 87 (2007) 2571–2588. https://doi.org/10.1080/14786430701241697

[29] U. Dey, N. Mitra, A. Taraphder, High temperature–high pressure phase transformation of Cu, Computational Materials Science, 170 (2019) 1-7. https://doi.org/10.1016/j.commatsci.2019.109154

[30] Y.Z. Yang, Y.M. Jiang, J. Li, In situ investigation of crevice corrosion on UNS S32101 duplex stainless steel in sodium chloride solution, Corrosion Science, 76 (2013) 163–169. https://doi.org/ 10.1016/j.corsci.2013.06.039

[31] C. Torres, R. Johnsen, M. Iannuzzi, Crevice corrosion of solution annealed 25Cr duplex stainless steels: Effect of W on critical temperatures, Corrosion Science, 178 (2021) 1-14. https://doi.org/ 10.1016/j.corsci.2020.109053

[32] M. Abdelbar, A.M. El-Shamy, Understanding soil factors in corrosion and conservation of buried bronze statuettes: insights for preservation strategies, Scientific Reports, 14 (2024) 1-28. https://doi.org/10.1038/s41598-024-69490-5

[33] J. Akpoborie, O.S. I. Fayomi, O. Agboola, O.D. Samuel, B.U. Oreko, A.A. Ayoola, Electrochemical corrosion phenomenon and prospect of materials selection in curtailing the challenges, Materials Science and Engineering, 1107 (2021) 1-10. https://doi.org/ 10.1088/1757-899x/1107/1/012072

[34] M.S. Anwar, T.B. Romijarso, E. Mabruri, Pitting resistance of the modified 13Cr martensitic stainless steel in chloride solution, International Journal of Electrochemical Science, 13 (2018) 1515–1526. https://doi.org/ 10.20964/2018.02.13

[35] V. Encinas-Sánchez, M.T. de Miguel, M.I. Lasanta, G. García-Martín, F.J. Pérez, Electrochemical impedance spectroscopy (EIS): An efficient technique for monitoring corrosion processes in molten salt environments in CSP applications, Solar Energy Materials and Solar Cells, 191 (2019)157–163. https://doi.org/10.1016/j.solmat.2018.11.007

[36] M. Swayne, G. Perumal, D.B. Padmanaban, D. Mariotti, D. Brabazon, Exploring the impact of laser surface oxidation parameters on surface chemistry and corrosion behaviour of AISI 316L stainless steel, Applied Surface Science Advances, 22 (2024) 1-13. https://doi.org/ 10.1016/j.apsadv.2024.100622

UTICAJ TEMPERATURE TOPLOG VALJANJA NA MIKROSTRUKTURU I OTPORNOST NA KOROZIJU SUPER DUPLEKS NERĐAJUĆEG ČELIKA KORIŠĆENOG ZA PREVLAČENJE NISKOUGLJENIČNOG ČELIKA U OKRUŽENJU MORSKE VODE

L. Naffat [a,*], M.S. Anwar [a], P.A. Paristiawan [a], A.N. Syahid [a], R.N. Hakim [a], Y. Lestari [a], M. Perkasa [b], K. Prijono [c]

[a] Istraživački centar za metalurgiju, Nacionalna agencija za istraživanje i inovacije (BRIN), Južni Tangerang, Džakarta, Indonezija

[b] Laboratorija za čvrstoću konstrukcija, Nacionalna agencija za istraživanje i inovacije (BRIN), Južni Tangerang, Džakarta, Indonezija

[c] Laboratorija za naprednu hemijsku i naprednu fiziku, Nacionalna agencija za istraživanje i inovacije (BRIN), Južni Tangerang, Džakarta, Indonezija

Apstrakt

Novi materijal koji se može koristiti kao zamena za pojedinačni čelik u sudovima visoke čvrstoće je niskougljenični čelik obložen Super Duplex nerđajućim čelikom (SDSS). Metod proizvodnje višeslojnog Super Duplex nerđajućeg čelika (SDSS) sastoji se u oblaganju niskougljeničnog čelika. Sprovode se mnogi procesi, poput zavarivanja pomoću plazma direktne energetske depozicije (DED), lasera i zavarivanja elektro-šljakom. U proizvodnoj industriji, toplo valjanje je jednostavan proces. Budući da je postupak brz i koristi jeftinu, tradicionalnu opremu, naziva se jednostavnom metodom. Korišćenje morske vode je odabrano jer slani uslovi pogoduju koroziji. U ovom radu se istražuju efekti temperatura od 900°C, 1000°C i 1050°C na mikrostrukturu i otpornost na koroziju toplo valjanih materijala. Glavni cilj ovog rada je ispitivanje otpornosti na koroziju analizom mikrostrukture i svojstava materijala korišćenjem metalografije, rendgenske difrakcije, elektroskopije elektrohemijske impedanse (EIS) i skenirajućeg elektronskog mikroskopa (SEM). Rezultati istraživanja su pokazali da sa povećanjem temperature toplog valjanja dolazi do karbonizacije i dekarbonizacije, a otpornost na koroziju se smanjuje.

Ključne reči: *SDSS; Niskougljenični čelik; Toplo valjanje; Karbonizacija; Dekarbonizacija*